

**$E2$  transitions in Sn isotopes within the quasiparticle-phonon model**N. Lo Iudice,<sup>1,\*</sup> Ch. Stoyanov,<sup>2,†</sup> and D. Tarpanov<sup>2</sup><sup>1</sup>*Dipartimento di Scienze Fisiche, Università di Napoli “Federico II” and Istituto Nazionale di Fisica Nucleare, Monte S. Angelo, Via Cintia, I-80126 Napoli, Italy*<sup>2</sup>*Institute for Nuclear Research and Nuclear Energy, Bulgarian Academy of Sciences, BG-1784 Sofia, Bulgaria*  
(Received 11 July 2011; revised manuscript received 18 September 2011; published 17 October 2011)

The evolution of the structure of the first  $2_1^+$  state along the chain of Sn isotopes is investigated within the quasiparticle-phonon model through the analysis of the energies and the  $B(E2; 0_1^+ \rightarrow 2_1^+)$  strengths. The calculation reproduces the trend of the energies and, partly, the observed deviations of the  $E2$  strengths from the parabolic behavior obtained in some large-scale shell-model calculations. Such an asymmetric trend is shown to be the outcome of several factors: single-particle energies, polarization of the  $N = Z = 50$  core, interplay between pairing plus quadrupole, and quadrupole pairing interactions.

DOI: [10.1103/PhysRevC.84.044314](https://doi.org/10.1103/PhysRevC.84.044314)

PACS number(s): 21.10.Pc, 21.10.Re, 21.60.Ev, 27.60.+j

**I. INTRODUCTION**

A series of experiments [1–7], mainly based on Coulomb excitation, have shown that the  $B(E2, 0_1^+ \rightarrow 2_1^+)$  reduced strengths along the chain of the Sn isotopes deviate from the parabolic trend, with a peak at midshell, predicted by the single  $j$ -shell seniority model [8]. The observed  $E2$  strengths have a parabolic trend only for  $A > 116$ . In the lighter isotopes, instead, the strength increases in going from  $A = 116$  to  $A = 114$ , and then remains roughly constant within the experimental uncertainties.

The data could not be described by a shell-model calculation performed in a space enlarged so as to promote the excitations of four protons from  $g_{7/2}$  to the valence shells ( $g_{7/2}, d_{5/2}, d_{3/2}, s_{1/2}$ ) [2]. It was found that the computed  $E2$  strengths still fall on a parabola peaked at  $A = 116$ .

The failure of the shell model in reproducing the  $B(E2)$  strengths along the Sn isotopic chain has raised doubts about the  $Z = N = 50$  shell closure. It should be said, however, that some asymmetry could be obtained within a shell-model approach using a  $G$  matrix derived from realistic two-nucleon potentials and including core polarization terms up to both the third order and  $5\hbar\omega$  core excitations [5].

The experimental situation is also in evolution. Two new experiments were performed at the Universal Linear Accelerator (UNILAC) of the GSI [9]. The data were analyzed in conjunction with those obtained in a recent magnetic-moment measurement [10] at the Australian National University (ANU).

In these new experiments [9], different  $B(E2)$  values were deduced for the stable  $^{112-124}\text{Sn}$  isotopes from direct measurements of the lifetimes of the first excited  $2^+$ . A shallow minimum at midshell was observed, followed by a smooth increase up to  $A = 112$  and  $A = 120$  in the lighter and heavier regions, respectively.

The trend followed by the new data deviates even more markedly from the shell-model predictions [2]. More promising is the description obtained in a relativistic, self-consistent, quasiparticle random-phase approximation (QRPA) approach [11,12]. The transition strength so computed decreases from a peak around  $A = 106$  up to midshell, remains nearly constant up to  $A = 124$ , and, finally, decreases until  $A = 130$ . The calculations reproduce well the data in the light and heavy isotopes and undermines the strengths around  $^{116}\text{Sn}$ .

A more phenomenological nonrelativistic QRPA calculation using a separable quadrupole-quadrupole plus quadrupole pairing potential is successful in reproducing the experimental trend for  $A > 116$  [13]. This calculation, unfortunately, was not extended to the lighter region.

Here we study these transitions within the quasiparticle-phonon model (QPM) [14]. This approach is based on the use of a Hamiltonian of general separable form. It has, therefore, a phenomenological character compared to the self-consistent QRPA approaches [11,12]. On the other hand, it includes up to six quasiparticle configurations allowing one to investigate the role of configurations not taken into account in QRPA. Moreover, its separable structure allows one to analyze the role of each different multipole piece in determining the properties of the  $2^+$  states. It might therefore render the data more intelligible and provide useful hints to less phenomenological approaches. Moreover, it allows one to cover a configuration space of arbitrarily large dimensions, which is of great relevance to the issue concerning the closure of the  $Z = N = 50$  shell.

**II. DETAILS OF THE CALCULATION**

The QPM Hamiltonian  $H_{\text{QPM}}$  is composed of a Woods-Saxon, one-body piece,

$$H_0 = T + V_{\text{WS}}, \quad (1)$$

plus a two-body potential, which is the sum of separable multipole terms acting in the particle-particle ( $p$ - $p$ ) and

\*loiodice@na.infn.it

†stoyanov@inrne.bas.bg

particle-hole ( $p$ - $h$ ) channels. Its explicit expression is

$$V = \sum_{\lambda} \kappa_{\lambda}(\tau\tau') Q_{\lambda}^{\dagger}(\tau) \cdot Q_{\lambda}(\tau') + \sum_{\lambda} G_{\lambda}(\tau) P_{\lambda}^{\dagger}(\tau) \cdot P_{\lambda}(\tau), \quad (2)$$

where  $\tau = \pi, \nu$ ,

$$Q_{\lambda}^{\dagger} \cdot Q_{\lambda} = \sum_{\mu} Q_{\lambda\mu}^{\dagger} Q_{\lambda-\mu} (-)^{\lambda-\mu}, \quad (3)$$

$$P_{\lambda}^{\dagger} \cdot P_{\lambda} = \sum_{\mu} P_{\lambda\mu}^{\dagger} P_{\lambda-\mu} (-)^{\lambda-\mu},$$

and

$$Q_{\lambda\mu}^{\dagger} = \sum_{qq'} \langle q | R(r) Y_{\lambda\mu}(\hat{r}) | q' \rangle a_q^{\dagger} a_{q'}, \quad (4)$$

$$P_{\lambda\mu}^{\dagger} = \sum_{qq'} \langle q | R(r) Y_{\lambda\mu}(\hat{r}) | q' \rangle a_q^{\dagger} a_{q'}^{\dagger},$$

are, respectively, the  $p$ - $p$  and  $p$ - $h$  multipole operators. The radial component is  $R(r) = dV_{WS}/dr$ , except for the monopole ( $\lambda = 0$ ) pairing for which a constant strength  $G_0$  is assumed. It is to be noticed that the  $p$ - $p$  potential is a sum of multipole pairing acting among proton or neutron pairs only.

The Hamiltonian is first used to generate the QRPA phonons

$$O_{i\lambda\mu}^{\dagger} = \frac{1}{2} \sum_{jj'} \{ \psi_{jj'}^{i\lambda} [\alpha_j^{\dagger} \alpha_{j'}^{\dagger}]_{\lambda\mu} - (-1)^{\lambda-\mu} \varphi_{jj'}^{i\lambda} [\alpha_j \alpha_j]_{\lambda-\mu} \} \quad (5)$$

of energies  $\omega_{i\lambda}$ . It is then expressed in terms of the above phonons assuming the form

$$H_{\text{QPM}} = \sum_{i\lambda\mu} \omega_{i\lambda} O_{i\lambda\mu}^{\dagger} O_{i\lambda\mu} + H_{vq}. \quad (6)$$

The first term is harmonic in the  $O_{i\lambda\mu}^{\dagger}$  QRPA phonon operators, and the second is a phonon-coupling piece whose exact expression can be found in Ref. [14]. In this phonon form, the Hamiltonian can be easily diagonalized in a space spanned by states composed of one, two, and three QRPA phonons.

The parameters of the Hamiltonian were determined according to a procedure well established in the QPM [14–17], which yields a well-defined set of parameters for all nuclei of a given nuclear mass region that is valid for high- as well as low-energy spectroscopic studies.

The parameters of the Woods-Saxon potential, shown in Table I, were taken from Refs. [18,19]. They were fixed by a systematic fit of binding energies, radii, spin-orbit splittings, and energies of the odd neighbors in the region. The single-particle energies and states so generated can be found in Ref. [17]. They span a space which encompasses all

TABLE I. The Woods-Saxon parameters for protons  $\tau = \pi$  and neutrons  $\tau = \nu$ . The numbers in parentheses are the values used for  $A > 118$ .

$\tau$	$r_0$ (fm)	$V_0$ (MeV)	$\kappa$ (fm <sup>2</sup> )	$\alpha$ (fm <sup>-1</sup> )
$\nu$	1.28	44.28 (43.20)	0.413	1.613
$\pi$	1.24	54.55 (59.90)	0.347	1.587

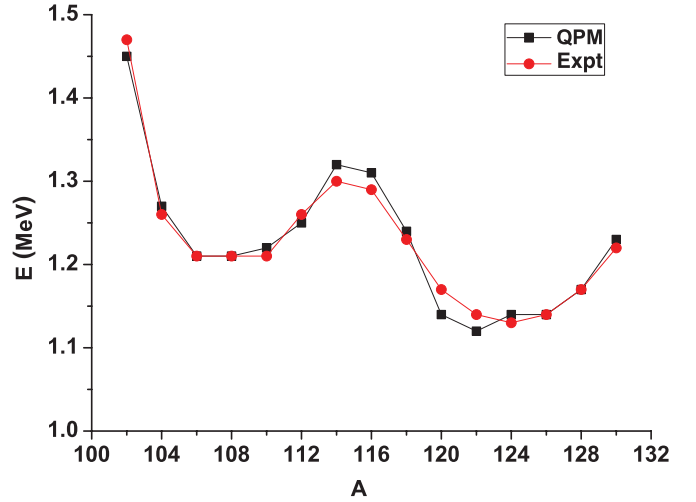


FIG. 1. (Color online) QPM vs experimental energies of the  $2_1^+$  states. The data are taken from Ref. [26].

shells from the bottom of the well up to the quasibound states embedded into the continuum, thereby allowing one to include core excitations of very high energy.

The monopole pairing constant is fixed by a fit of the odd-even mass differences. We found that  $G_0 = 0.14$  MeV for  $A \leq 118$  and  $G_0 = 0.125$  MeV for the heavier isotopes.

All  $\kappa_{\lambda}$  constants are in fm<sup>2</sup> MeV<sup>-1</sup>. The strengths  $\kappa_2$  and  $\kappa_3$  of the  $p$ - $h$  quadrupole-quadrupole and octupole-octupole potentials were determined by a fit to the energies of the first  $2_1^+$  and  $3_1^-$  states.

The isoscalar quadrupole constants resulted in  $\kappa_2(T = 0) = 0.016$  for  $A \leq 118$  and  $\kappa_2(T = 0) = 0.014$  for  $A > 118$ . For the octupole strength, we obtained  $\kappa_3(T = 0) = 0.016$  over the entire range. The octupole term, however, plays a negligible role.

The strengths  $\kappa_{\lambda}$  of the other multipole terms were adjusted so as to leave unchanged the energy of the computed lowest two-quasiparticle states [17]. We give as typical value the hexadecapole constant  $\kappa_4(T = 0) = 0.011$ .

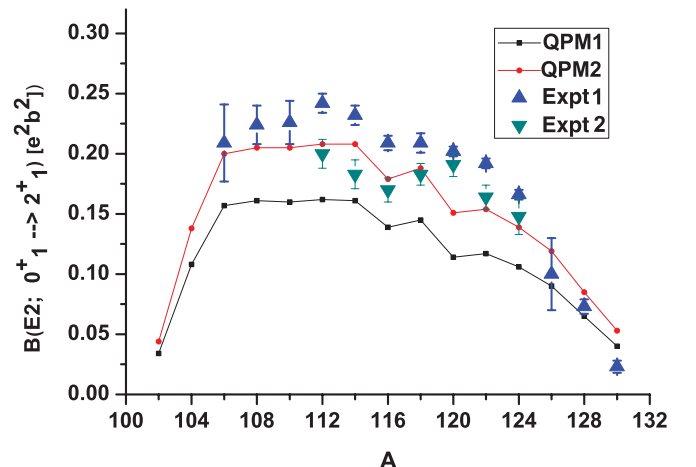


FIG. 2. (Color online) QPM vs experimental  $B(E2; 0_1^+ \rightarrow 2_1^+)$ .

TABLE II. Energy,  $E2$  strengths, weight of one-phonon ( $W_\lambda$ ) component in the QPM states, and weight of protons ( $W_\pi$ ) in the phonon. The QPM1 and QPM2  $B(E2)$  strengths were computed using, respectively, bare and effective charges ( $e_\pi = 1.05e$ ,  $e_\nu = 0.05e$ ). The Expt1 data are taken from Ref. [7], where the values of neutron-deficient isotopes were obtained by averaging over the measurements of Refs. [1–3,5]. The Expt2 data are taken from Ref. [9].

Nucleus	$E$ (MeV)		$W_\lambda$ %	$W_\pi$ %	QPM1	QPM2	$B(E2)(e^2b^2)$	
	QPM	Expt.					Expt1	Expt2
102	1.46	1.4720(2)	97	1.4	0.034	0.044		
104	1.27	1.2601(3)	93	4.3	0.108	0.138		
106	1.21	1.2077(5)	91	6.3	0.157	0.200	0.209(32)	
108	1.21	1.2061(2)	92	6.3	0.161	0.205	0.224(16)	
110	1.22	1.2119(2)	94	6.8	0.160	0.205	0.226(18)	
112	1.25	1.2569(7)	96	6.8	0.162	0.208	0.242(8)	0.195(8)
114	1.32	1.2999(7)	98	6.8	0.161	0.208	0.232(8)	0.186(8)
116	1.31	1.2936(8)	99	6.0	0.139	0.179	0.209(6)	0.170(10) <sup>a</sup> /0.165(10) <sup>b</sup>
118	1.24	1.2297(2)	98	6.0	0.145	0.188	0.209(8)	0.183(9)
120	1.14	1.1713(2)	97	4.3	0.114	0.151	0.202(4)	0.191(10)
122	1.12	1.1406(3)	98	4.1	0.117	0.154	0.192(4)	0.164(10)
124	1.14	1.1317(2)	98	4.0	0.106	0.139	0.166(4)	0.148(15)
126	1.15	1.1412(2)	97	3.7	0.090	0.119	0.10(3)	
128	1.17	1.1688(4)	96	2.6	0.065	0.085	0.073(6)	
130	1.23	1.1213(5)	95	1.5	0.040	0.053	0.023(5)	

<sup>a</sup>GSI value.

<sup>b</sup>ANU value.

The isovector strengths are taken to be  $\kappa_\lambda(T=1) = -1.2\kappa_\lambda(T=0)$ , as is common practice in QPM.

The  $\lambda \neq 0$  multipole pairing terms are necessary to restore the Galilean invariance [20–22]. Among them, only the quadrupole pairing is relevant to low-energy spectra and, in particular, is of crucial importance for describing the so-called mixed symmetry states [23,24]. It is shown there that a strength of the order  $G_2 \sim \kappa_2$  is necessary in order to generate a sufficiently collective mixed symmetry  $2^+$  state. The same constant was adopted in deformed nuclei to study, for instance, the properties of the  $0^+$  states in the nuclei of the rare-earth and actinide region [25]. We put, therefore,  $G_2 = \kappa_2$ .

We stress that the fit was done within the QPM. The calculation showed that the  $2^+$  states are sensitive only to the monopole pairing, quadrupole-quadrupole, and quadrupole pairing terms.

### III. ANALYSIS OF THE RESULTS

The QPM  $2_1^+$  levels are fully consistent with the data (Fig. 1). The analysis of the  $E2$  transitions is more problematic. As shown in Fig. 2, both old (Expt1) and new (Expt2) data are underestimated by the QPM calculation using bare effective charges (QPM1).

A better agreement with the data, especially the new ones (Expt2), is achieved if we use effective charges slightly larger than the bare values ( $e_\pi = 1.05e$ ,  $e_\nu = 0.05e$ ) (QPM2). These small corrections to the bare charges are to be included in the calculation. They incorporate the core polarizations contributions, which cannot be taken into account in a mean-field approach no matter how large the configuration space is. In fact, effective charges ranging between

( $e_\pi = 1.05e$ ,  $e_\nu = 0.05e$ ) and ( $e_\pi = 1.1e$ ,  $e_\nu = 0.1e$ ) have always been used in QPM calculations.

In both cases, the QPM  $E2$  strengths follow a trend consistent with the experimental values. In fact, the calculation yields a dip at  $A = 116$  and an enhancement around and below the midshell, consistently with the data. Such a behavior could only be obtained once the configuration space was enlarged so as to account explicitly for the excitations of the nucleons, especially the protons, of the  $N = Z = 50$  core. The core polarization is more pronounced in the lighter isotopes, where the enhancement of the  $E2$  transition strengths is observed. As shown in Table II, the weight of the protons in each  $2^+$  state is between 6 and 7% in the isotopes up to  $A = 118$  and falls to 2–4% in the heavier isotopes.

A minor role is played by the multiphonon components. The two-phonon content is always small and becomes negligible as we move away from the neutron shell closures (Table II). We can then conclude that the  $2_1^+$  states are basically one-phonon states.

Though crucial for reproducing the data, the core component represents a modest share of each phonon (Table III). This gets reflected in the weak collectivity of the  $2_1^+$  states, made manifest by their high excitation energies if compared to the corresponding levels of the neighbor nonmagic nuclei, and by the small  $B(E2, 0_1^+ \rightarrow 2_1^+)$ , exhausting only a few percent of the  $E2$  sum rule [26].

The behavior of the energies and strengths shown above is the outcome of a subtle interplay between the different pieces of the Hamiltonian.

Since the neutron pairing gap increases as we approach the neutron midshell, the neutron two-quasiparticle energies get higher and approach the proton two-quasiparticle levels, which are not affected by the neutrons and, therefore, remain

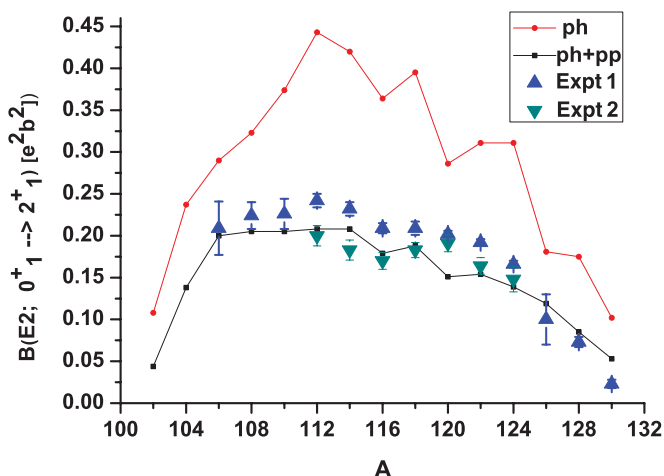
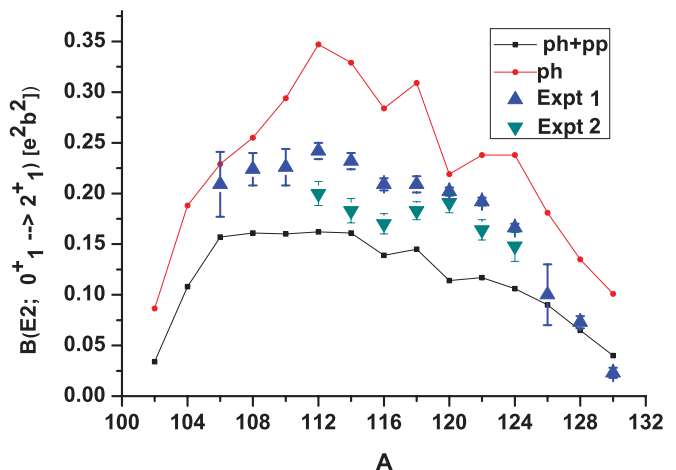
TABLE III. Quasiparticle composition of the  $2_1^+$  state in two typical Sn isotopes.

Nucleus	$(q_1q_2)_v$	$W_{q_1q_2}^{(v)}$ (%)	$(q_1q_2)_{pi}$	$W_{q_1q_2}^{(\pi)}$ (%)
$^{112}\text{Sn}$	$1g_{7/2}1g_{7/2}$	20.6	$1g_{9/2}2d_{5/2}$	5
	$1h_{11/2}1h_{11/2}$	16	$1g_{9/2}1i_{13/2}$	0.6
	$1g_{7/2}2d_{3/2}$	17		
	$2d_{5/2}3s_{1/2}$	11.7		
	$2d_{5/2}2d_{5/2}$	5.6		
	$3s_{1/2}2d_{3/2}$	6		
	$2d_{3/2}2d_{3/2}$	2.5		
	$2d_{5/2}2d_{3/2}$	2.5		
$^{126}\text{Sn}$	$1h_{11/2}1h_{11/2}$	61	$1g_{9/2}2d_{5/2}$	2.6
	$2d_{3/2}2d_{3/2}$	8.1		
	$3s_{1/2}2d_{3/2}$	9.3		
	$1g_{7/2}2d_{3/2}$	6.5		
	$1h_{11/2}2f_{7/2}$	3.1		

constant along the chain. It follows that the  $p$ - $h$  quadrupole interaction becomes more effective and enhances the weight of the protons in the structure of the first  $2^+$ . Thus, as we move toward the neutron midshell, the  $E2$  strength increases due to the increasing collectivity of the proton component of the  $2^+$ .

The above remarks suggest that the monopole pairing plus the  $p$ - $h$  quadrupole interaction favor a parabolic behavior of the  $B(E2)$  up to  $A = 116$ . Figure 3 shows that this is the case. Substantial deviations from a parabola are observed in the heavier isotopes. The asymmetry with respect to midshell is due to the fact that the Woods-Saxon parameters change in moving from  $A \leq 118$  to  $A > 118$ , generating two distinct sets of single-particle energies. It might be worthwhile to stress once again that this parametrization was determined independently of the present calculation.

The figure shows that pairing plus quadrupole yield a too large  $E2$  strength for all isotopes even with bare


 FIG. 3. (Color online)  $B(E2; 0_1^+ \rightarrow 2_1^+)$  with and without quadrupole pairing with effective charges  $e_\pi = 1.05e$ ,  $e_\nu = 0.05e$ .

 FIG. 4. (Color online)  $B(E2; 0_1^+ \rightarrow 2_1^+)$  with and without quadrupole pairing with bare effective charges.

charges (Fig. 4). The  $B(E2)$  is drastically reduced once the quadrupole pairing is added. This particle-particle potential, in fact, enhances the weight of the neutron two-quasiparticle configurations at the expense of the protons' particle-hole states. The action of the quadrupole pairing is selective. It induces a different quenching of the  $E2$  transitions in different isotopes and has the effect of smoothing the behavior of the  $B(E2)$  with the mass number.

#### IV. CONCLUSION

In conclusion, the QPM describes partially the asymmetric behavior of the  $B(E2; 0_1^+ \rightarrow 2_1^+)$  transition strengths in the Sn isotopes with respect to the midshell, and yields also a minimum at  $A = 116$ .

The preliminary condition for getting the enhancement of the  $E2$  strength in the lighter tin region is to account explicitly for the excitations of the nucleons, especially the protons, of the  $N = Z = 50$  core. The core polarization is modest, nonetheless, it is a strong indication of the stability of the  $N = Z = 50$  shell closure. The role of complex configuration such as two- and three-phonon components is also marginal.

Several other factors enter into the process of bringing the theoretical quantities fairly close to the experimental data. One is the use of two distinct sets of single-particle energies for light and heavy Sn isotopes, respectively, which result from an *a priori* parametrization of the Woods-Saxon potential. The two sets suggest a different character of the two possible  $N = 50$  and  $N = 82$  neutron cores. Another factor is the combined action of pairing plus quadrupole, which determines an increasing weight of protons in the  $Z = 50$  core, with consequent enhancement of the  $E2$  strengths.

Finally, a crucial ingredient is represented by the quadrupole pairing. The fair agreement between the QPM and experimental observables, all along the Sn chain, could not be reached without the quenching and smoothing action of

this  $p$ - $p$  potential. Once again, quadrupole pairing appears to have a strong impact on the low-lying spectroscopic properties of complex nuclei, including nuclei away from the stability line.

#### ACKNOWLEDGMENT

One of the authors (Ch.S.) acknowledges the financial support from the INFN within the agreement between INFN and the Bulgarian Science Foundation.

- 
- [1] D. C. Radford *et al.*, *Nucl. Phys. A* **752**, 264c (2005).  
 [2] A. Banu *et al.*, *Phys. Rev. C* **72**, 061305(R) (2005).  
 [3] J. Cederkäll *et al.*, *Phys. Rev. Lett.* **98**, 172501 (2007).  
 [4] C. Vaman *et al.*, *Phys. Rev. Lett.* **99**, 162501 (2007).  
 [5] A. Ekstrom *et al.*, *Phys. Rev. Lett.* **101**, 012502 (2008).  
 [6] P. Doornenbal *et al.*, *Phys. Rev. C* **78**, 031303(R) (2008).  
 [7] R. Kumar *et al.*, *Phys. Rev. C* **81**, 024306 (2010).  
 [8] I. Talmi, *Simple Models of Complex Nuclei* (Harwood Academic, Chur, Switzerland, 1993).  
 [9] A. Jungclaus *et al.*, *Phys. Lett. B* **695**, 110 (2011).  
 [10] M. East *et al.*, *Phys. Lett. B* **665**, 147 (2008).  
 [11] A. Ansari, *Phys. Lett. B* **623**, 37 (2005).  
 [12] A. Ansari and P. Ring, *Phys. Rev. C* **74**, 054313 (2006).  
 [13] J. Terasaki, *Nucl. Phys. A* **746**, 583c (2004).  
 [14] V. G. Soloviev, *Theory of Atomic Nuclei : Quasiparticles and Phonons* (Institute of Physics Publishing, Bristol, 1992).  
 [15] M. Grinberg and Ch. Stoyanov, *Nucl. Phys. A* **535**, 231 (1994).  
 [16] V. Yu. Ponomarev, Ch. Stoyanov, N. Tsoneva, and M. Grinberg, *Nucl. Phys. A* **635**, 470 (1998).  
 [17] S. Gales, Ch. Stoyanov, and A. I. Vdovin, *Phys. Rep.* **166**, 125 (1988).  
 [18] V. A. Chepurnov, *Yad. Fiz.* **6**, 955 (1967) [*Sov. J. Nucl. Phys.* **6**, 696 (1968)].  
 [19] K. Takeuchi and P. A. Moldauer, *Phys. Lett. B* **28**, 384 (1969).  
 [20] S. T. Belyaev, *Yad. Fiz.* **4**, 936 (1966) [*Sov. J. Nucl. Phys.* **4**, 671 (1967)].  
 [21] H. Sakamoto and T. Kishimoto, *Phys. Lett. B* **245**, 321 (1990).  
 [22] T. Kubo, H. Sakamoto, T. Kammuri, and T. Kishimoto, *Phys. Rev. C* **54**, 2331 (1996).  
 [23] N. Lo Iudice and Ch. Stoyanov, *Phys. Rev. C* **65**, 064304 (2002).  
 [24] N. Lo Iudice and Ch. Stoyanov, *Phys. Rev. C* **69**, 044312 (2004).  
 [25] N. Lo Iudice, A. V. Sushkov, and N. Y. Shirikova, *Phys. Rev. C* **70**, 064316 (2004).  
 [26] S. Raman, C. W. Nestor Jr., and P. Tikkanen, *At. Data Nucl. Data Tables* **78**, 1 (2001).